COMPUTATIONAL MECHANICS
New Trends and Applications
E. Oñate and S.R. Idelsohn (Eds.)
©CIMNE, Barcelona, Spain 1998

ON THE USE OF FINITE ELEMENT MODELING TECHNIQUES TO REPRESENT ROTATING MACHINERY

C. A. Almeida and M. A. Meggiolaro
Pontificia Universidade Católica, R.J.
R. Marques de São Vicente, 225 - Gávea, Rio de Janeiro, Brasil
e-mail: calmeida@mec.puc-rio.br

Key words: Finite Element Techniques, Rotating Machinery, Hydrodynamics Bearings, Newmark Time Integration, Numerical Solution Evaluations.

Abstract. *In this work a formulation for the analysis of shaft-rotor-bearing type rotating systems is extended to accommodate the effects of hydrodynamics bearings in its dynamic response. These effects, which are associated to the nonlinear force on the shaft at the bearing, are dependent of the transverse displacements and rotations, transverse linear and angular velocities and the shaft angular velocity. The structure behavior is modeled by employing the finite element method. The shaft is represented by the two node Timoshenko model for beams, with four degrees-of-freedom per node and Hermite interpolation functions to represent the displacement fields along the beam axis. Rotors are modeled by using concentrated inertia elements associated to the degrees-of-freedom of one nodal point of the model. To represent the hydrodynamic bearings the equation of Reynolds was used under the simplified Ocvirk conditions for short bearings, providing a closed form solution for the oil film pressure distribution. This pressure distribution allows for the calculation of stiffness and damping matrices associated to the shaft degrees-of-freedom at the bearing nodal point. In the numerical analysis considering the time integration of the system differential equation, a step-by-step procedure was employed with the Newmark technique in its unconditionally form. Due to the nonlinearities associated with the hydrodynamic bearing, the solution of the system of equations is obtained using a modified Newton-Raphson procedure at each time for solution convergence. In the evaluation of the proposed computational system, comparison with solutions obtained from analytical/numerical results available in the literature are used. Also, a numeric representation of tilting-pad bearings is presented using the theory for plain journal bearing, under the same simplified conditions. In this case an evaluation of the numerical procedure is given by comparing calculated solutions with experimental results obtained from the analysis results of a hydrogeneration plant provided by CEPEL-Brazilian Research Center for Eletrotrobras. In both plain and tilting-pad journal bearing numerical procedures, the idealized Jeffcott rotor is employed as a case study for different operating conditions. As a result, it is shown that the solutions associated to the main oil whirl and oil whip effects and the afterwards dynamic stabilization are represented by the proposed numerical procedures employed.*

1. INTRODUCTION

The general area of rotordynamics has, at least historically, been the amalgam of knowledge from two very active research areas in Mechanical Engineering: structure dynamics and journal bearing oil film dynamics. It provides the frame work theory and simulation tools to represent the mechanical behaviour of rotatory systems, which are the main responsible machinery for transforming fluid potential energy (chemical, gravitational, etc) into rotatory kinetic energy, and vice versa. Hydrogenerators are good examples of these complex systems. They comprise, basically, four main components: the impeller, the shaft, the bearings and the seals. Mass umbalances as well as gravity must be also considered[1-3].

In the design process of hydrogenerators, requirements for mechanical performance and dynamic stability are, in general, conflictory. If, for its best performance, the largest as possible fluid flow passing the machine is a desirable operating condition, this may turn the machine, limited in size and weight, into an unstable system. Thus, in a hydrogenerator project, the following objectives may be perceived[3]:

- avoid to operate at critical speeds, if possible. Vibration mode exitations may cause the system to fail by ressonance;
- minimize the dynamic response at ressonance, in case of critical speeds being crossed during operation. This requires the analyst to have a good knowledge of the rotor dynamic behaviour;
- minimize random vibration loadings at the machine operating speeds. Undesirable oscilatory responses are avoided, by reducing external excitations;
- avoid dynamic unstabilities. Certain operation conditions may cause the system self-excited vibration motions, at amplitudes larger than it was primarily designed for;
- avoid torsional vibrations at ressonance. Flexural vibrations combined to the system response on the torsional modes at ressonance may be amplified to levels dangerous to the structure integrity.

In most of the operating field conditions, access to experimental results are useful to system design but, in general, difficult to obtain or, in some cases, not cost effective. Also, because the system dynamic response is not known in its design phase, suitable positions for the experimental pick up points are, generally, difficult to define. Figure 1 presents an assemblage part representation for a typical hydrogenerator and its third mode (amplified) response at 12.9 hz, with shaft angular velocity at 100 rpm. To evaluate the dynamics of such hydrogenerators, under the above operating conditions, a robust numerical procedure is required and the finite element method provides the adequate numerical tools. It has been extensively used in the literature to model the dynamic behaviour of nonlinear - geometric or material - structures[4-5] and, from the physics involved, rotating systems are adequately represented by beams and concentrated/distributed masses to represent shaft and rotors, respectively. However, modeling of the bearing influence on the structure dynamics requires some special considerations. By simply using decoupled spring constants its influence has been analytically evaluated in the literature[6-7]. Rao[8] extended these studies to evaluate their effects in the Jeffcott rotor at its critical speed by including the coupling terms

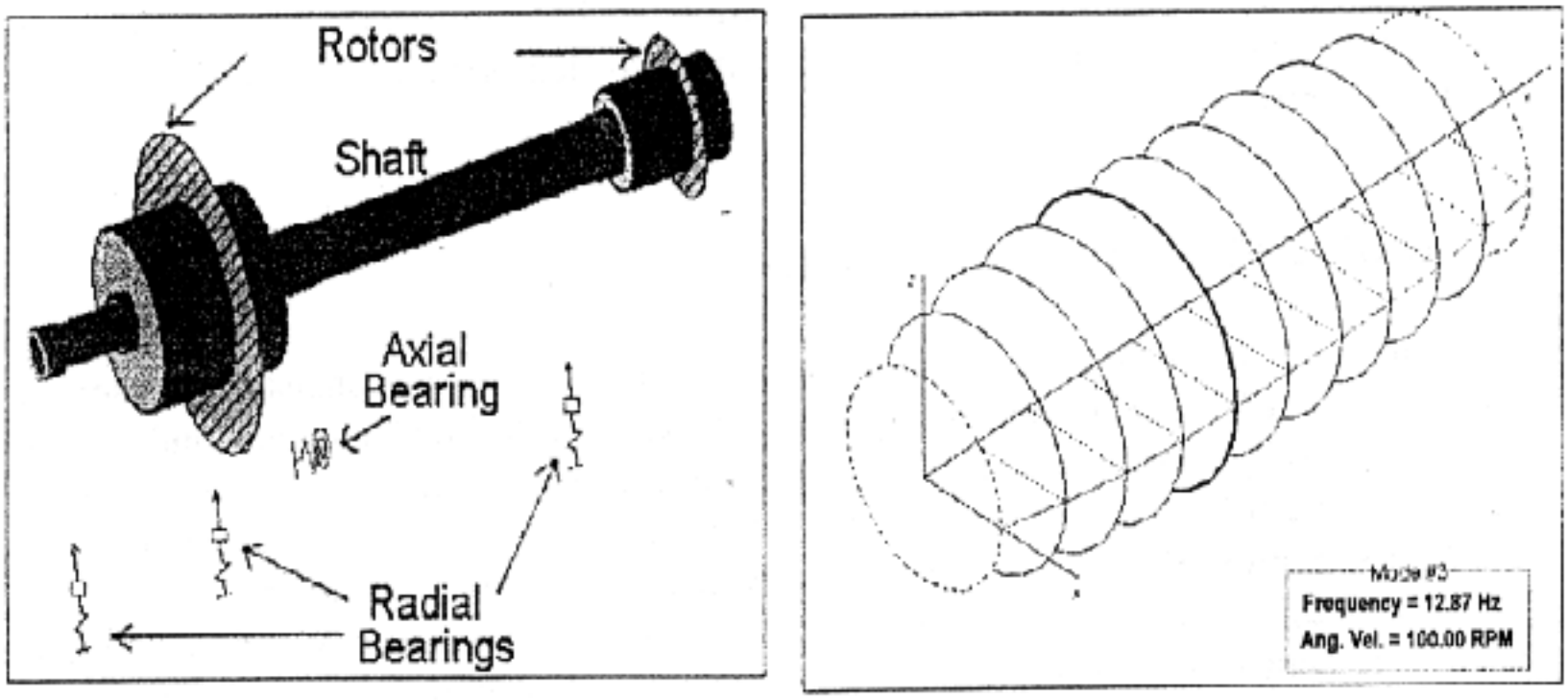

Figure 1 - Rotating System Components and Typical Mode Response

associated to hydrodynamic bearings. His study was further extended to consider damping effects in the bearing model[9]. It shows how damping can be a very important effect in the response of a rotating system subjected to unbalance forces, at its critical speed.

Due to these properties modern hydrogenerators employ low stiffness - such the oil film type - journal bearings. In these systems the largest amount of energy dissipation occurs at the bearings, which are the supporting devices mainly responsible for the supression of dynamic ressonance and for the reduction of sincronous response to umbalancing. Nonsimmetry and small coupling terms in the stiffness equivalent matrix are very important characteristics, to the system stability.[1-3]

In the present investigation, the finite element idealization is used as basic numerical procedure. The approach is similar in many respects to the formulations presented by Nicholas[10], except that a more general methodology is obtained in the representation of bearing support forces. The paper deals with the formulation of a simple but effective procedure for the dynamic response of rotating systems. The formulation procedures predict the significant phenomena occuring in rotordynamic systems including ressonance, oil whirl and oil whip effects, and the afterwards dynamic stabilization. Stiffness and damping matrices associated to the shaft motion in the bearing oil film are obtained in closed form, for each angular position of the shaft, by ensuring its dynamic equilibrium conditions. In this paper single-span/multi-rotor systems with perfectly aligned bearings are considered. However, the full potential of the procedure lies in the analysis of multi-span/multi-rotor systems with or without misligned bearings[11], because it is cost effective and indeed allows an accurate nonlinear dynamic analysis. This nonlinear effect, proper to multi-span systems, is ought to be included in a subsequent extension of the present work.

In the next section the important concepts used in the finite element representation of rotating systems are presented. Stiffness and damping matrices derivations associated to hydrodynamic bearings are presented in section 3. In this section plain and tilting pad type

bearings are both considered. The formulation has been implemented in the computer, and in section 4 some analysis results are presented to demonstrate the validity of the proposed numerical procedures.

2. SHAFT AND ROTOR FE MODELS

The analysis of a general assemblage of finite elements consists, in essence, of the formulations of the equilibrium equations of each individual element and the subsequent application of general procedures that are independent of the type of element considered. Hence, in the following discussion we will focus on the derivations of typical elements for the representation of the shaft, rotor and bearings in rotating machinery.

The Shaft Model. Considering the shaft structural behavior we adopt the Timoshenko beam element model formulation. It consists of a two-node element with the assumption that plane sections originally normal to the beam neutral axis remain plane, but because of shear deformations it does not remain perpendicular to the neutral axis. The approach requires, to represent the element kinematics, four degrees-of-freedom per node - two transverse v and w displacements and two in-plane rotations β_1 and β_2. Thus, for a shaft of length L laying in the z-direction axis and subjected to the angular velocity $\dot{\phi}$, the element total potential is given by

$$\pi = (EI/2)\int_0^L[(\partial\beta_1/\partial z)^2) + (\partial\beta_2/\partial z)^2]\,dz + (kGA/2)\int_0^L[(\partial v/\partial z + \beta_1)^2 + (\partial w/\partial z - \beta_2)^2]\,dz - \\ -(\rho I_0/2)\int_0^L\dot{\phi}(\dot{\beta}_1\beta_2 + \dot{\beta}_2\beta_1)\,dz + (F/2)\int_0^L[(\partial v/\partial z)^2 + (\partial w/\partial z)^2]\,dz \qquad (1)$$

where the first two integrals are, respectively, bending and shearing strain energies and the last two integrals represent the potential of the gyroscope moment- due to angular velocity combinations-and the potential of an axial load F, respectively. The upper dot (•) on the variable implies differenciation with respect to time. In eq. (1) E, ρ and G are, respectively, the material Young's modulus, mass density and shear modulus, while A, I and I_0 are the cross-section geometric parameters: area, transverse moment of inertia and polar moment of inertia, respectively.

In order to include the shaft dynamic behaviour in the formulation, also its kinetic energy must be considered. Thus, we have

$$V_c = (\rho/2)\left[\int_0^L A(\dot{v}^2 + \dot{w}^2)dz + \int_0^L I(\dot{\beta}_1^2 + \dot{\beta}_2^2)dz + \int_0^L I_0\dot{\phi}^2 dz\right] \qquad (2)$$

where the first two terms are the kinetic energies due to transverse displacements and rotations of the beam cross-section, and the remaining is due to the shaft spin. Under the small displacement condition the third integral in equation (1) may be reduced to the form

$$(\rho I_0) \int_0^L \dot{\phi}\dot{\beta}_1\beta_2 \, dz . \qquad (3)$$

Also, it is worthed to notice that the strain energy term in eq. (1) associated to the axial load F is an important term when vertical rotor assemblages are considered with axial bearings in its lower position. This axial strain energy is thus significative, compared to bending and shearing straining energies, for the case in which the total turbine weight added to the water flow pressure is about twenty times the rotor own weight[12] .

In the above equations all the element state variables are represented along the shaft axis, only. In this case, Hermitian cubic polinomial are employed as interpolation functions in the z-direction. As an example, the transverse v - displacement representation results in

$$v(z) = [1 - 3(z/L)^2 + 2(z/L)^3]v_1 + [3(z/L)^2 - 2(z/L)^3]v_2 \qquad (4)$$

with v_1 and v_2 being the element nodal point displacements. This numerical representation is then extended to all state variables which combined to eqs. (1), (2) and (3) results, after integration, in the element stiffness, damping and consistent mass matrices, all obtained in closed form[12].

The Rotor Model. As a machinery component to store kinetic (rotating) energy, which is obtained from the combination of three angular motions: spin, precession and nutation, the analyst is required to distinguish, in the finite element model representation of a rotor, the use of the consistent or the lumped mass representation. In general, consistent mass models are required in "long rotors" representation larger than one-tenth of the shaft's length. In this case the rotor may be modeled as a beam element and eqs. (1) to (3) apply. In the second representation, proper to "short rotors" the lumped mass model is employed, associated to the degrees-of-freedom at a single node of the shaft representation. In this case the kinetic energy to be added to the finite element representation at node N, is given by

$$V_L = (M_R/2)(\dot{v}_M^2 + \dot{w}_M^2) + (I_R/2)(\dot{\beta}_{1N}^2 + \dot{\beta}_{2N}^2) + (I_{OR}/2)(\dot{\phi}^2 + 2\dot{\beta}_{2N}\dot{\phi}\beta_{1N}) \qquad (5)$$

where M_R, I_R and I_{OR} are, respectively, the rotor total mass, the rotor mass moment of inertia with respect to x-axis and the rotor mass moment of inertia with respect to z-axis.

In both formulations the equivalent damping matrix obtained from the potential due angular velocity combination - the gyroscope moment -, in eq. (3), results in an anti-symmetric matrix. This implies the dynamic systems to possess 2n natural frequencies, for each shaft angular velocity $\dot{\phi}$. These frequencies are upper and lower bounds of n natural frequencies obtained from a stand shaft ($\dot{\phi} = 0$) and they correspond to fast and slow procession solutions.

3. HYDRODYNAMIC BEARINGS

Hydrodynamic bearings such as journal bearings are used to support rotors. Because it allows for the dissipation of kinetic energy in the shaft, it also provides rotor damping to either assist in stabilizing an otherwise unstable rotor or to improve synchronous response characteristics. Although simpler to be manufactured as compared to others, plain journal bearings are subject to dynamic unstabilities due to self-exercited precessions. Tilting pad journals, on the other hand, provide a substantial reduction in this unpleasant rotor response because the cross-coupling terms in the equivalent bearing-stiffness matrix is substantially reduced. In this section derivations for the equivalent stiffness and damping matrices associated to these two types of hydrodynamic bearing are presented.

Plain Bearings. Hydrodynamic bearing reaction forces acting on rotating shafts result from the pressure developed by the relative motion of, assumed parallel, surfaces retaining a thin oil film. Considering the Reynolds equations, in convective coordinates, representing an incompressible Newtonian fluid under laminar flow conditions, with no body forces present but constant viscosity, the pressure field $p(\theta, z)$ in the bearing results from[1]

$$\frac{\partial}{\partial\theta}(h^3\frac{\partial p}{\partial\theta}) + R^2\frac{\partial}{\partial Z}(h^3\frac{\partial p}{\partial Z}) = 12\mu(\frac{R}{C_r})^2(\frac{\omega}{2}\frac{\partial h}{\partial\theta} + \frac{\partial h}{\partial t}), \quad 0 \le z \le \ell \qquad (6)$$

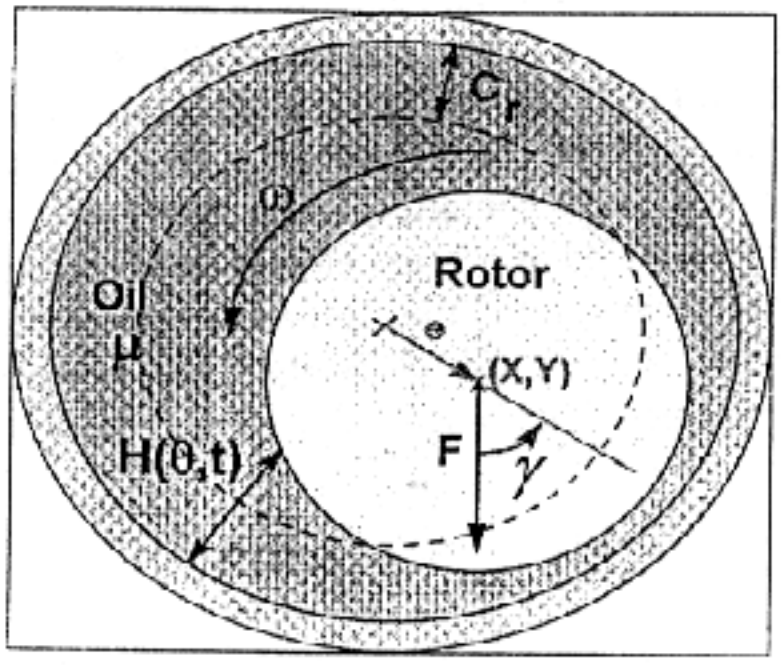

Figure 2 - Plain Bearing Physical and Geometric Parameters

where ω is the rotor angular velocity, $\varepsilon = e / C_r$ is the rotor normalized excentricity, C_r is the radial clearance, $h(\theta,t) = H(\theta, t) / C_r$ is the instant normalized clearance along the bearing circunference and R is the shaft radius. Closed form solutions for eq. (6) can be obtained for two simplified conditions only[13]: long and short bearings. In the former the resulting pressure gradiente in the axial z-direction is much smaller than the pressure gradient in the circunferential θ-direction. This condition results the second term on the left hand

side of eq. (6) negligible, compared to the others. It will not be considered here, since hydrogenerators employ, in general, hydrodynamic bearings with aspect ratio (ℓ / R) less than 0.5[1]. Under short bearing conditions, on the other hand, the pressure gradient in the circunferential direction is negligible and the Reynolds equation results in,

$$C_r^2 \frac{\partial}{\partial Z}\left(h^3 \frac{\partial p}{\partial Z}\right) = 12\mu\left(\frac{\omega}{2}\frac{\partial h}{\partial \theta} + \frac{\partial h}{\partial t}\right) \tag{7}$$

with the pressure field solution

$$p(\theta, z) = (3\mu\omega/4)(\ell/C_r^2)\left[(x-2\dot{y})\sin\theta - (y+2\dot{x})\cos\theta\right](4z^2-1)/h^3 \tag{8}$$

defined from the non-dimensional parameters

$$x = \frac{X}{C_r} \quad ; \quad y = \frac{Y}{C_r} \quad ; \quad z = \frac{Z}{L} \quad ; \quad \dot{x} = \frac{\partial X/\partial t}{\omega C_r} \quad ; \quad \dot{y} = \frac{\partial Y/\partial t}{\omega C_r} \tag{9}$$

Negative values for $p(\theta, z)$ indicates the occurrence of cavitation in the oil film, and the pressure distribution is thus assumed null at $\alpha - \pi \le \theta \le \alpha$, with

$$\alpha = \mathrm{tg}^{-1}\frac{(y+2x)}{(x-2y)} - \frac{\pi}{2}\,\mathrm{sign}\,\frac{(y+2\dot{x})}{(x-2\dot{y})} - \frac{\pi}{2}\,\mathrm{sign}(y+2\dot{x}), \tag{10}$$

which is known as Gümbel condition for π-bearings.

From the pressure distribution in the oil film, reaction forces at the bearings are obtained by integrating $p(\theta, z)$, in eq. (8), over the shaft wet area $-0.5 < z < 0.5$ and $\alpha < \theta < \pi + \alpha$,[14,15]

$$\overline{F} = \begin{Bmatrix} F_x \\ F_y \end{Bmatrix} = -\left[\iint p(z,\theta)\begin{Bmatrix}\cos\theta \\ \sin\theta\end{Bmatrix}(R\partial\theta)(\partial z)\right] = -k\frac{n}{m}\overline{W} \tag{11}$$

where

$$\begin{aligned}
&k = \mu\omega\frac{R\ell^3}{4C^2} \quad , \quad u = y + 2\dot{x} \quad , \quad v = x - 2y \\
&n = \sqrt{u^2+v^2} \quad , \quad m = 1 - x^2 - y^2 \quad , \quad \alpha = \mathrm{tg}^{-1}\left(\frac{u}{v}\right) - \frac{\pi}{2}\,\mathrm{sign}(u) \\
&p = y\cos\alpha - x\sin\alpha \, , \quad q = x\cos\alpha + y\sin\alpha \, , \quad \overline{W} = \begin{Bmatrix} 3xV - G\sin\alpha - 2F\cos\alpha \\ 3yV + G\cos\alpha - 2F\sin\alpha \end{Bmatrix} \\
&V = \frac{2 + pG}{m} \quad , \quad G = \frac{\pi}{\sqrt{m}} + \frac{2}{\sqrt{m}}\mathrm{tg}^{-1}\left(\frac{p}{\sqrt{m}}\right) \quad , \quad F = \frac{q}{1-q^2}
\end{aligned} \tag{12}$$

Stiffness and damping matrices coefficients are obtained from the derivatives of these force components with respect $x, y, \dot{x}, \dot{y}$. Thus,

$$\begin{bmatrix} K_{xx} \\ K_{yx} \end{bmatrix} = - \frac{\partial \overline{F}}{\partial X} = \left(k \left(\frac{v}{mn} + \frac{2xn}{m^2} \right) \overline{W} + k \frac{n}{m} \frac{\partial \overline{W}}{\partial x} \right) \frac{1}{C_r}$$

$$\begin{bmatrix} K_{xy} \\ K_{yy} \end{bmatrix} = - \frac{\partial \overline{F}}{\partial Y} = \left(k \left(\frac{u}{mn} + \frac{2yn}{m^2} \right) \overline{W} + k \frac{n}{m} \frac{\partial \overline{W}}{\partial y} \right) \frac{1}{C_r}$$

$$\begin{bmatrix} C_{xx} \\ C_{yx} \end{bmatrix} = - \frac{\partial \overline{F}}{\partial \dot{x}} = \left(k \frac{2u}{m\,n} \overline{W} + k \frac{n}{m} \frac{\partial \overline{W}}{\partial \dot{x}} \right) \frac{1}{\omega C_r} \qquad (13)$$

$$\begin{bmatrix} C_{xy} \\ C_{yy} \end{bmatrix} = - \frac{\partial \overline{F}}{\partial \dot{y}} = \left(- k \frac{2v}{mn} \overline{W} + k \frac{n}{m} \frac{\partial \overline{W}}{\partial \dot{y}} \right) \frac{1}{\omega C_r}$$

In eqs. (13) derivatives of $\overline{W}$ are given by

$$\frac{\partial \overline{W}}{\partial x} = \begin{Bmatrix} 3V + 3x \frac{\partial V}{\partial x} - G \cos\alpha \frac{\partial \alpha}{\partial x} - \frac{\partial G}{\partial x} \sin\alpha + 2F \sin\alpha \frac{\partial \alpha}{\partial x} - 2 \frac{\partial F}{\partial x} \cos\alpha \\ 3y \frac{\partial V}{\partial x} - G \sin\alpha \frac{\partial \alpha}{\partial x} + \frac{\partial G}{\partial x} \cos\alpha - 2F \cos\alpha \frac{\partial \alpha}{\partial x} - 2 \frac{\partial F}{\partial x} \sin\alpha \end{Bmatrix}$$

$$\frac{\partial \overline{W}}{\partial y} = \begin{Bmatrix} 3x \frac{\partial V}{\partial y} - G \cos\alpha \frac{\partial \alpha}{\partial y} - \frac{\partial G}{\partial y} \sin\alpha + 2F \sin\alpha \frac{\partial \alpha}{\partial y} - 2 \frac{\partial F}{\partial y} \cos\alpha \\ 3V + 3y \frac{\partial V}{\partial y} - G \sin\alpha \frac{\partial \alpha}{\partial y} + \frac{\partial G}{\partial y} \cos\alpha - 2F \cos\alpha \frac{\partial \alpha}{\partial y} - 2 \frac{\partial F}{\partial y} \sin\alpha \end{Bmatrix}$$

$$\frac{\partial \overline{W}}{\partial \dot{x}} = \begin{Bmatrix} 3x \frac{\partial V}{\partial \dot{x}} - G \cos\alpha \frac{\partial \alpha}{\partial \dot{x}} - \frac{\partial G}{\partial \dot{x}} \sin\alpha + 2F \sin\alpha \frac{\partial \alpha}{\partial \dot{x}} - 2 \frac{\partial F}{\partial \dot{x}} \cos\alpha \\ 3y \frac{\partial V}{\partial \dot{x}} - G \sin\alpha \frac{\partial \alpha}{\partial \dot{x}} + \frac{\partial G}{\partial \dot{x}} \cos\alpha - 2F \cos\alpha \frac{\partial \alpha}{\partial \dot{x}} - 2 \frac{\partial F}{\partial \dot{x}} \sin\alpha \end{Bmatrix} \qquad (14)$$

$$\frac{\partial \overline{W}}{\partial \dot{y}} = \begin{Bmatrix} 3x \frac{\partial V}{\partial \dot{y}} - G \cos\alpha \frac{\partial \alpha}{\partial \dot{y}} - \frac{\partial G}{\partial \dot{y}} \sin\alpha + 2F \sin\alpha \frac{\partial \alpha}{\partial \dot{y}} - 2 \frac{\partial F}{\partial \dot{y}} \cos\alpha \\ 3y \frac{\partial V}{\partial \dot{y}} - G \sin\alpha \frac{\partial \alpha}{\partial \dot{y}} + \frac{\partial G}{\partial \dot{y}} \cos\alpha - 2F \cos\alpha \frac{\partial \alpha}{\partial \dot{y}} - 2 \frac{\partial F}{\partial \dot{y}} \sin\alpha \end{Bmatrix}$$

Furthermore, the following set of derivative definitions, with respect to $x, y, \dot{x}$, and $\dot{y}$, are also needed in the calculations shown in eq. (14):

- Derivatives of α:

$$\frac{\partial \alpha}{\partial x} = \frac{-u}{u^2 + v^2}, \quad \frac{\partial \alpha}{\partial y} = \frac{v}{u^2 + v^2}, \quad \frac{\partial \alpha}{\partial \dot{x}} = \frac{2v}{u^2 + v^2}, \quad \frac{\partial \alpha}{\partial \dot{y}} = \frac{2u}{u^2 + v^2} \tag{15}$$

- Derivatives of V:

$$\frac{\partial V}{\partial x} = \frac{\left[p\frac{\partial G}{\partial x} - \left(q\frac{\partial \alpha}{\partial x} + \sin\alpha\right) G\right] m + 2x(2 + p.G)}{m^2}$$

$$\frac{\partial V}{\partial y} = \frac{\left[p\frac{\partial G}{\partial y} - \left(q\frac{\partial \alpha}{\partial y} - \cos\alpha\right) G\right] m + 2y(2 + p.G)}{m^2} \tag{16}$$

$$\frac{\partial V}{\partial \dot{x}} = \frac{\left[p\frac{\partial G}{\partial \dot{x}} - q\frac{\partial G}{\partial \dot{x}} G\right]}{m} \quad ; \quad \frac{\partial V}{\partial \dot{y}} = \frac{\left[p\frac{\partial G}{\partial \dot{y}} - q\frac{\partial \alpha}{\partial \dot{y}} G\right]}{m}$$

- Derivatives of G:

$$\frac{\partial G}{\partial x} = \frac{x}{m\sqrt{m}}\left(\pi + 2tg^{-1}\left(\frac{p}{\sqrt{m}}\right)\right) + 2\frac{\frac{px}{m} - q\frac{\partial \alpha}{\partial x} - \sin\alpha}{m + p^2}$$

$$\frac{\partial G}{\partial y} = \frac{y}{m\sqrt{m}}\left(\pi + 2tg^{-1}\left(\frac{p}{\sqrt{m}}\right)\right) + 2\frac{\frac{py}{m} - q\frac{\partial \alpha}{\partial x} - \cos\alpha}{m + p^2} \tag{17}$$

$$\frac{\partial G}{\partial \dot{x}} = \frac{-2q\frac{\partial \alpha}{\partial \dot{x}}}{m + p^2} \quad ; \quad \frac{\partial G}{\partial \dot{y}} = \frac{-2q\frac{\partial \alpha}{\partial \dot{y}}}{m + p^2}$$

- Derivatives of F:

$$\frac{\partial F}{\partial x} = \left(p\frac{\partial \alpha}{\partial x} + \cos\alpha\right)\frac{(1+q^2)}{(1-q^2)^2} \qquad \frac{\partial F}{\partial y} = \left(p\frac{\partial \alpha}{\partial y} + \sin\alpha\right)\frac{(1+q^2)}{(1-q^2)^2}$$

$$\frac{\partial F}{\partial \dot{x}} = p\frac{\partial \alpha}{\partial \dot{x}}\frac{(1+q^2)}{(1-q^2)^2} \quad ; \quad \frac{\partial F}{\partial \dot{y}} = p\frac{\partial \alpha}{\partial \dot{y}}\frac{(1+q^2)}{(1-q^2)^2} \quad : \tag{18}$$

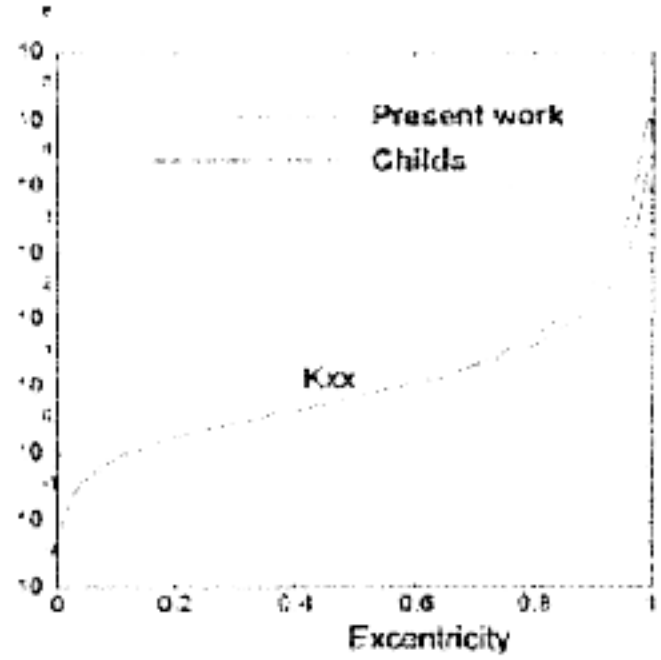

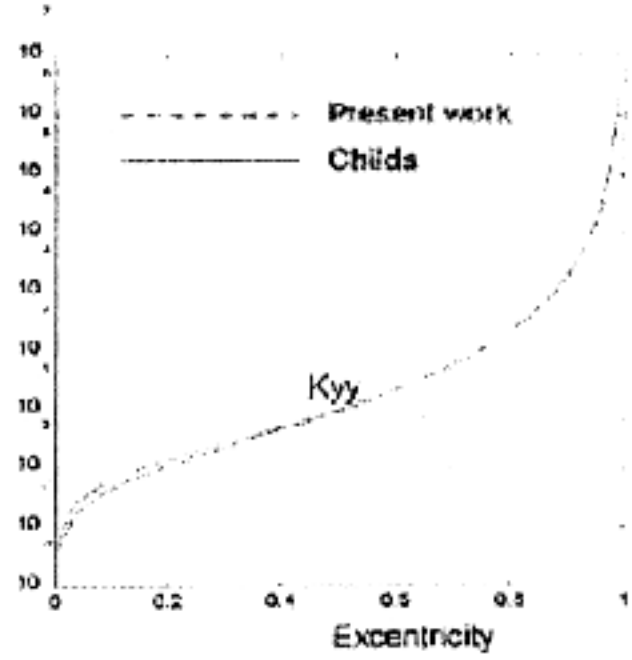

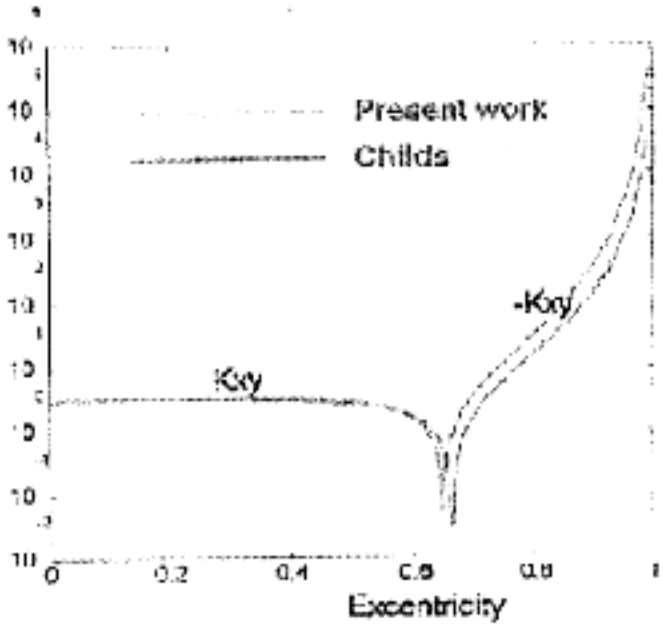

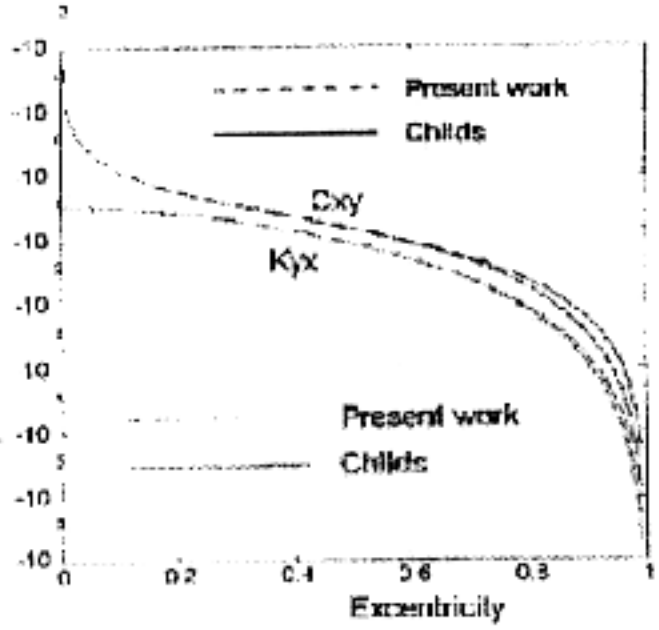

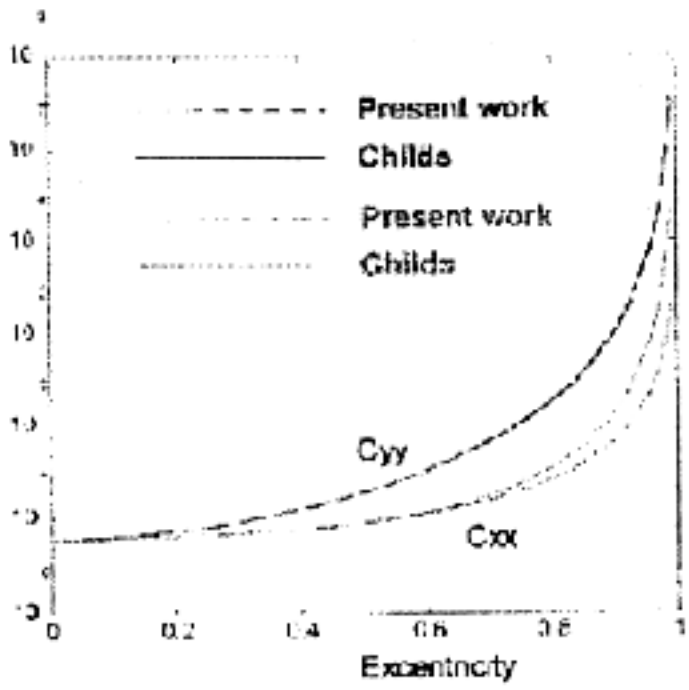

Figure 3 - Calculated Stiffness and Damping Coefficients for Plain Bearings, with $\dot{\phi} = 0$

From eqs. (13) to (18) the obtained stiffness and damping matrix coefficients depends on the bearing dimensions, the oil viscosity, the rotor angular velocity and the position and the precession velocity of the shaft with respect to the bearing case. These coefficients are plotted in Fig. 3, for null precession velocities, and compared to Childs[1] with respect to the excentricity parameter ε. The obtained model results presented in this work are more general because the shaft precession velocities are not neglected in the calculations and the x-y positions considered correspond to a general rotor configuration. From the plots, significative differences in some coefficients are noticed for ε >0.7. However, typical hydrogenerator rotors carry excentricity less than 0.3 and, in this range, good agreement is obtained in all result comparisons. The non-symmetry characteristic of the stiffness matrix is also shown in the results as well as that it increases for increasing bearing excentricity. On the other hand the damping matrix presents symmetry with strong coupling coefficients.

Tilting-Pad Bearings. The tilting-pad bearing design eliminates bearing-stability difficulties by eliminating the stiffness cross-coupling terms in the bearing representation. Considering the lower pads of tilting-pad bearing shown in Fig. 4, these pads are pivoted by an axial pin, which does not support moment; hence, the force reaction on the pads must pass through the pivot point, and a vertical load applied to the journal must be, for equilibrium, the sum of the reaction forces in both pins. The important physical point is that reaction forces are developed without sideward displacements of the loaded journal; i.e. a vertical load yields only a vertical displacements and the cross-coupling term in the equivalent stiffness matrix is then eliminated. Tilting-pad bearings have been used in hydrogenerator assemblies with 3,4, 5, 6, 12 and up to 18 pads.

Considering (x,y) coordinates of the rotor center, with respect to the bearing center, the oil film thickness, for a θ_0 angular position of the pin, may be obtained, see Fig. 5 as

$$h(\theta,\psi) = C_r - X\cos\theta - Y\sin\theta - \psi\sqrt{x_{X0}^2 + Y_0^2}\,\sin(\theta - \theta_0) \qquad (19)$$

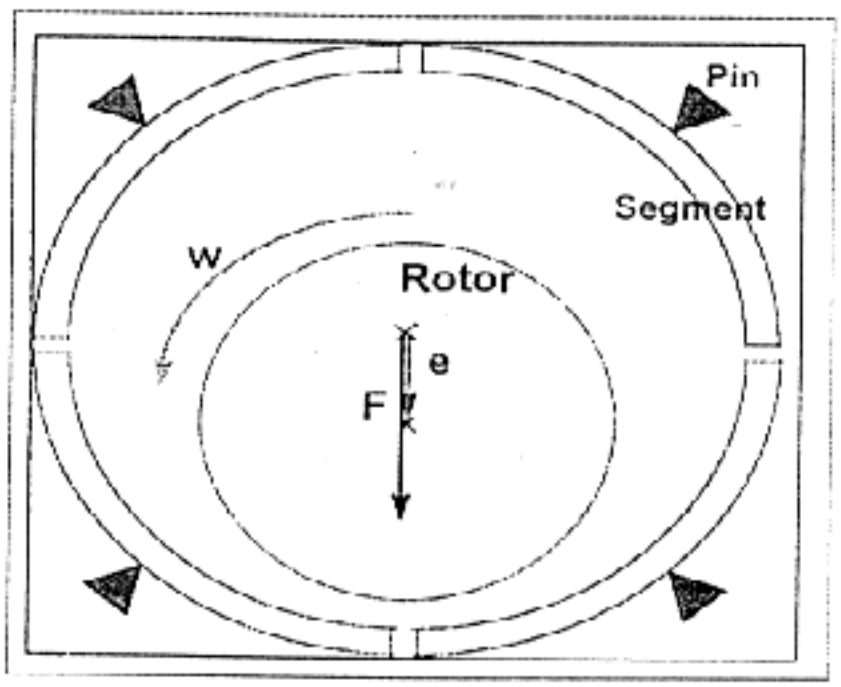

Figure 4 - Tilting-Pad Bearing Components

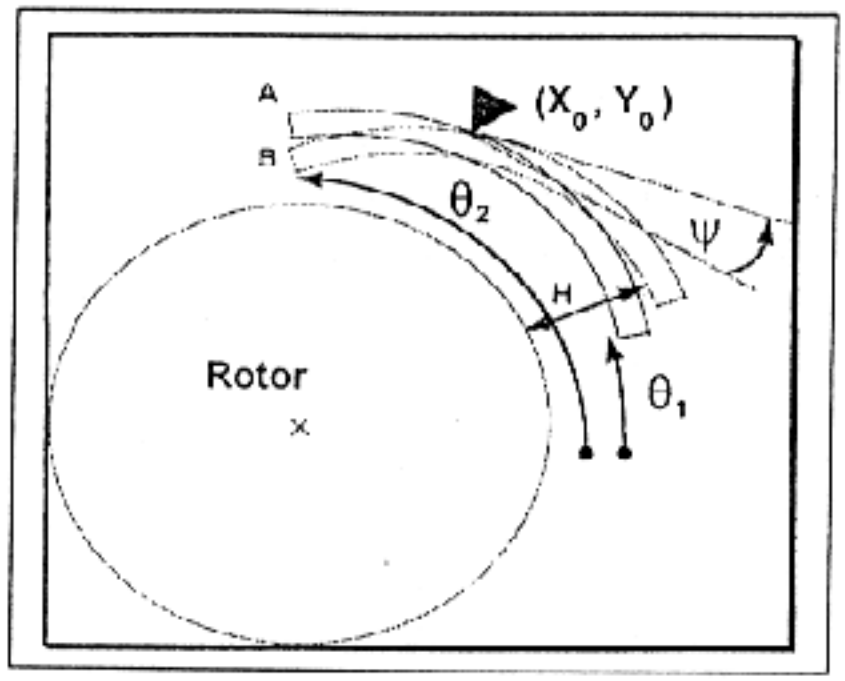

Figure 5 - Bearing Pad Relative Position Coordinates

Pressure distribution in each pad (segment) may be then obtained from the Reynolds equation - as Ocvirk conditions apply[1] - resulting in

$$p(\theta, z) = (3\mu\omega / 4)\,(\ell / C_r)^2\,[(a - 2\dot{b})\sin\theta - (b + 2\dot{a})\cos\theta]\,(4z^2 - 1)/h^3 \qquad (20)$$

where, $a = x - \psi Y_0 / C_r$, $b = y + \psi X_0 / C_r$ and the notation $(\dot{\bullet}) = \frac{1}{\omega}\frac{\partial}{\partial t}$ applies.

As in eq. (20), force components are evaluated for $\theta_1 < \theta < \theta_2$, resulting in

$$\overline{F} = \begin{Bmatrix} F_x \\ F_y \end{Bmatrix} = k \begin{Bmatrix} v.I_2 - u.I_1 \\ v.I_3 - u.I_2 \end{Bmatrix} \qquad (21)$$

where, $k = \mu\omega \dfrac{R\ell^3}{4C_r^2}$, and

$$I_1 = \int \frac{2\cos^2\theta}{h^3}\,d\theta, \quad I_2 = \int \frac{2\sin\theta\,\cos\theta}{h^3}\,d\theta, \quad I_3 = \int \frac{2\sin^2\theta}{h^3}\,d\theta \qquad (22)$$

Closed forms for the integral terms in eq. (20) are obtained through auxiliary algebraic transformations, which result in the following[12]

$$I_1 = \frac{G}{m} + \frac{3a}{m}\frac{\partial G}{\partial x} + \frac{2}{m}\frac{tg(\theta/2)-b}{q} + 2\left(\frac{a.G}{m} - \frac{\partial G}{\partial x}\right)\frac{p.tg(\theta/2)-a}{q}\Bigg|_{\theta_1}^{\theta_2}$$

$$I_2 = \frac{a}{m}\frac{\partial G}{\partial y} + \frac{2b}{m}\frac{\partial G}{\partial x} - \frac{2}{m}\frac{2b.tg(\theta/2)+a}{q} - 2\left(\frac{a.G}{m} - \frac{\partial G}{\partial x}\right)\frac{p+b}{q}\Bigg|_{\theta_1}^{\theta_2} \qquad (23)$$

$$I_3 = \frac{G}{m} + \frac{3b}{m}\frac{\partial G}{\partial y} + \frac{2}{m}\frac{p+b}{q} - 2\left(\frac{b.G}{m} - \frac{\partial G}{\partial y}\right)\frac{p+b}{q}\Bigg|_{\theta_1}^{\theta_2}$$

with,

$$G = \frac{2}{\sqrt{m}}\left(\text{arctg}\,\frac{p}{\sqrt{m}} + \text{int}\left(\frac{\theta+\pi}{2\pi}\right)\right) \qquad (24)$$

In the evaluation of the angular position ψ, for each bearing pad, the moment equilibrium condition due to oil film pressure is imposed. The resulting equation is numerically integrated in the time domain as described in Cardinali[13].

Following the procedures described for plain journal bearings, stiffness and damping matrix coefficients are then obtained from derivations of force components in eq. (19) with respect to x,y - coordinate components and $\dot{x}$, $\dot{y}$ - velocity components. Thus,

$$K_{xx} = -\frac{\partial F_x}{\partial X} = -\frac{k}{C_r}\left(v.\frac{\partial I_2}{\partial x} - u.\frac{\partial I_1}{\partial x} + I_2\right)$$

$$K_{xy} = -\frac{\partial F_x}{\partial Y} = -\frac{k}{C_r}\left(v.\frac{\partial I_2}{\partial y} - u.\frac{\partial I_1}{\partial y} - I_1\right)$$

$$K_{yx} = -\frac{\partial F_y}{\partial X} = -\frac{k}{C_r}\left(v.\frac{\partial I_3}{\partial x} - u.\frac{\partial I_2}{\partial x} + I_3\right)$$

$$K_{yy} = -\frac{\partial F_y}{\partial Y} = -\frac{k}{C_r}\left(v.\frac{\partial I_3}{\partial y} - u.\frac{\partial I_2}{\partial y} - I_2\right)$$

$$C_{xx} = -\frac{\partial F_x}{\partial \dot{X}} = \frac{2k}{\omega C_r} I_1$$

$$C_{xy} = -\frac{\partial F_x}{\partial \dot{Y}} = \frac{2k}{\omega C_r} I_2 \qquad (25)$$

$$C_{yx} = -\frac{\partial F_y}{\partial \dot{X}} = \frac{2k}{\omega C_r} I_2$$

$$C_{yy} = -\frac{\partial F_y}{\partial \dot{Y}} = \frac{2k}{\omega C_r} I_3$$

are evaluated for each segment and the resulting stiffness and damping matrices are obtained by adding up contributions of all bearing pads. As in previous derivations the integration domain is restrited to the pad region under positive values only of the pressure distribution, described in eq. (20). Also, in the time integration considered, the inertia moments associated to the angular motion of the pad is assumed negligible compared to all other forces considered in the equilibrium of the bearing pad.

4. ANALYSIS RESULTS

The foregoing formulation has been implemented and in this section the analysis responses predicted using finite element procedures are compared to available numerical/experimental results. In all analysis the equilibrium equations are numerically integrated in the time domain using the Newmark procedures, in its unconditionally stable form (α= 0,25, γ= 0,5). As presented, the formulation does not employ numerical integration schemes in space domain.

Analysis of a Rotor Assemblage with Plain Hydrodynamic Bearing. Figure 6 shows a vertical flexible rotor supporting a disk on its lower end while a motor is attached to the upper end. This assemblage was numerically evaluated by Lima[16] and the finite element model employed within this study are shown in Fig. 6. The obtained numerical solutions for the orbit patterns described by the shaft, at the bearing position - node 4 - are shown in Fig 7 for two rotor speeds: 30 rd/s and 100rd/s. Because the hydrodynamic bearings are

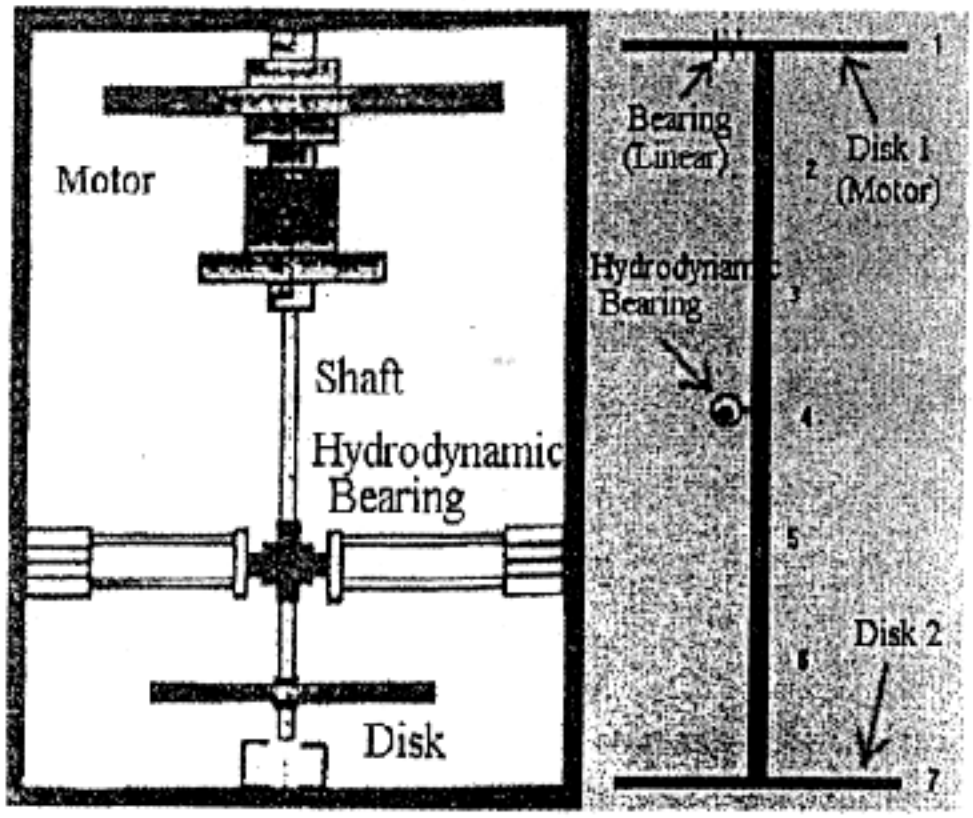

Figure 6 - Vertical Rotor Assemblage and The Finite Element Model Used

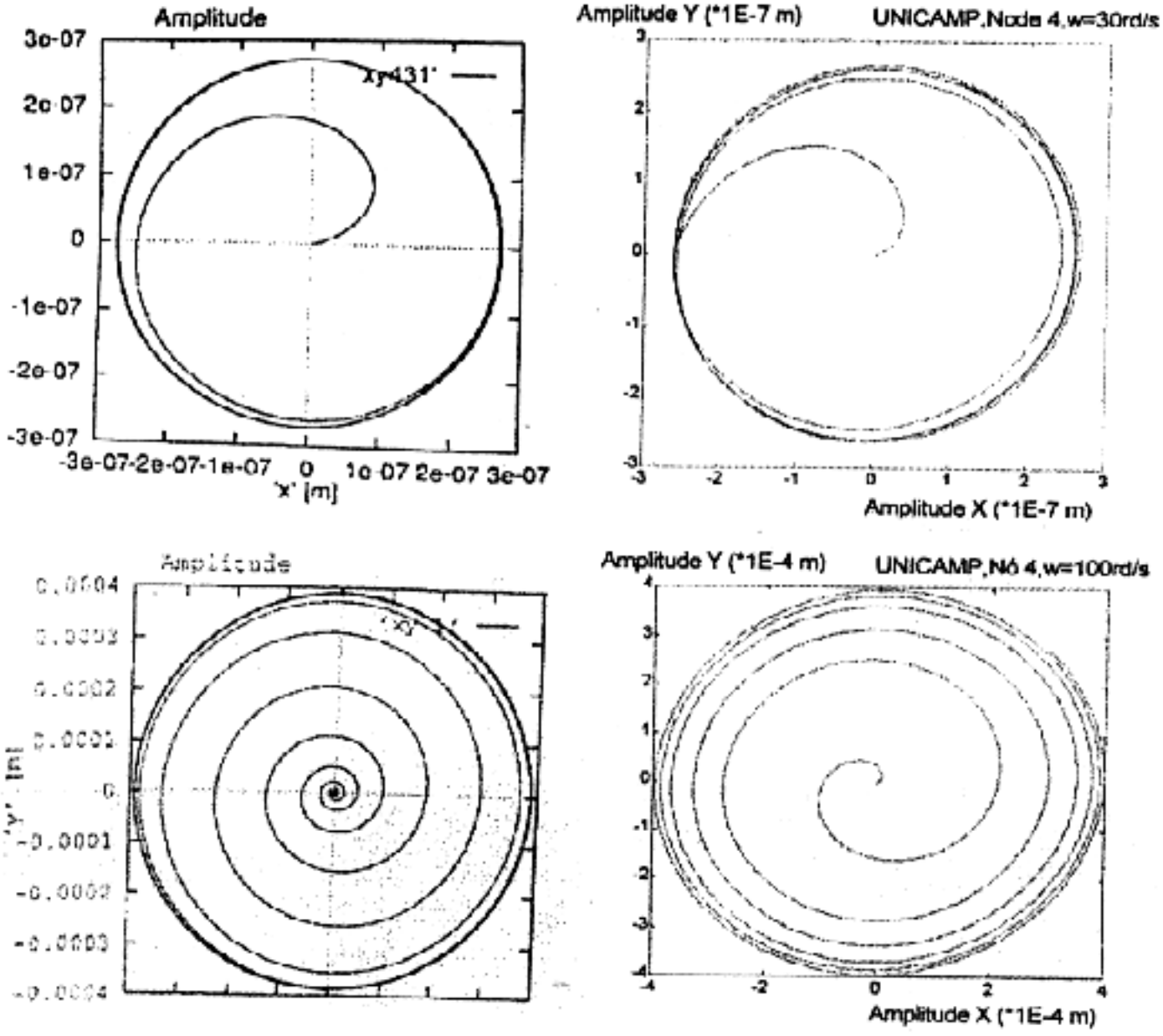

Figure 7 - Shaft Orbits Numerically Obtained Using: Present Study (Left) and Lima' Model (Right)

already incorporated to the model, in the present study, the time step used during integration of the equilibrium equations could be fifty times larger than the one used by Lima - $\Delta t = 2. \times 10^{-5} s$. In his analysis, the bearing was modeled by an equivalent reaction force model which required an explicity procedure to obtain the pressure integration domain considered in the analysis. At the steady-state motion of the rotor, solution trajectories obtained by Lima are similar to the ones generated by the present model. However they possess some differences due to the representation of the exciting force caused by shaft unbalancing. In our model instead of using a step loading, a slow exponential time increasing function was employed to avoid numerical unstabilities in the solution.

Analysis of a Rotor with Tilting-Pad Bearing. In this study the unit of Furnas Hydro-Power System, located at the southern part of Rio de Janeiro state, was considered. Experiments have been conducted and analized for further predictory maintenance planning

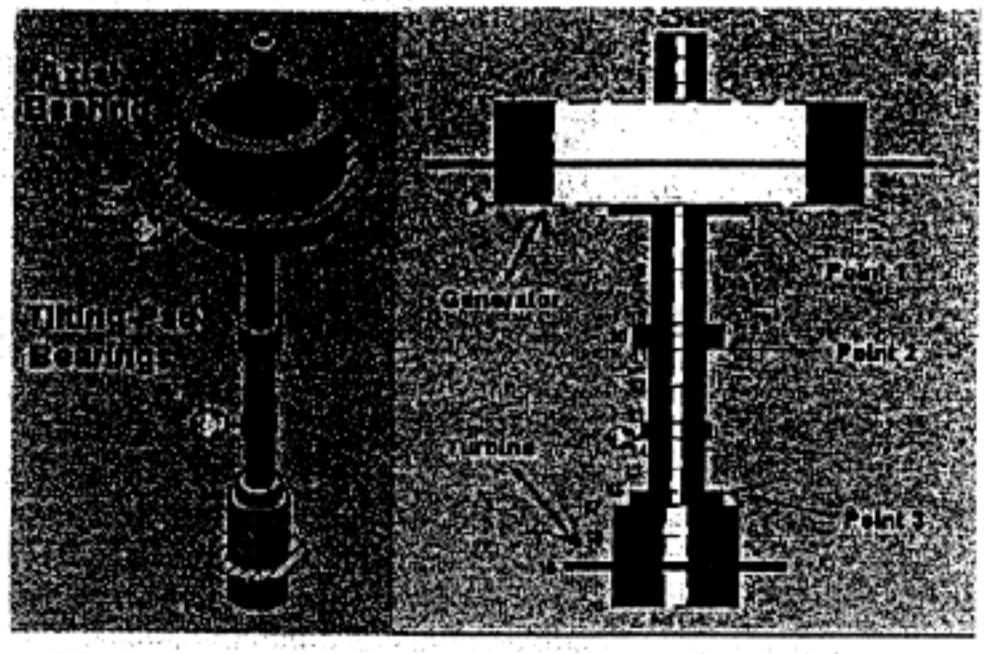

Figure 8 - Furnas Hydro-Power System Components and the Finite Element Model Employed

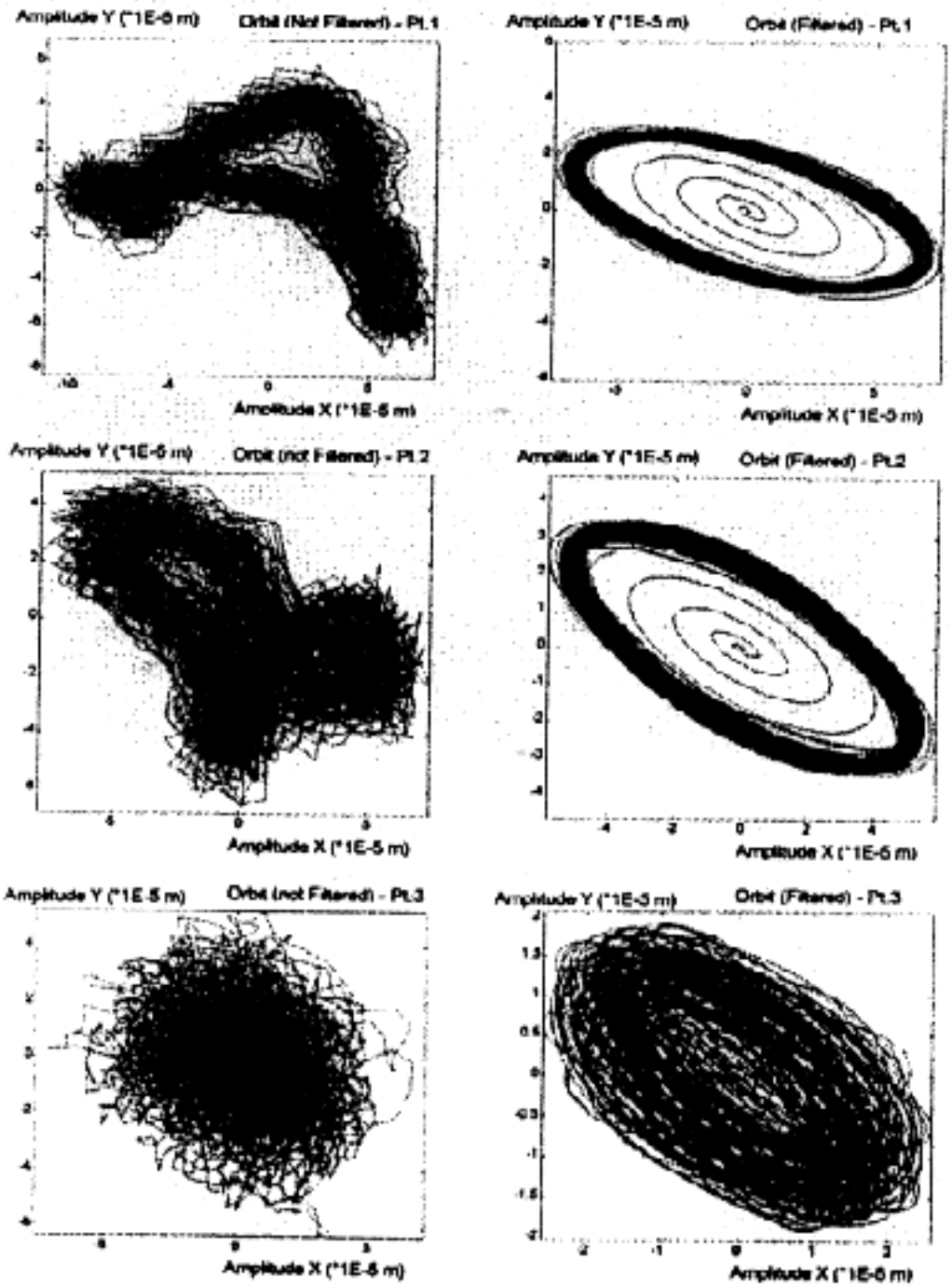

Figure 9 - Measured Shaft Orbits at the Pick Up Points: Before (Left) and After (Right) Filtering

by CEPEL (Brazilian Research Center for Eletrobras). In the numerical analysis the rotor was modeled using 19 Hermetian beam elements with two disk elements to represent the unit generator and the turbine, two tilting-pad bearing models as lateral bearings and one axial (trust) bearing. In this analysis the axial force due to the equipment weight had to be considered. Measured rotor orbits were obtained by using displacement transducers placed on the shaft axis at the position nodes 6,11 and 16. Figure 8 presents the system components and its finite element representation. Due to external excitation such as unbalancing forces, electric-magnetic forces and so on, measurement signs were filtered by a digital an eliptic type, 4th order filter with a 2.3 - 2.7hz pass band and low band cut of 100 db. All data were obtained for the rotor at 150 rpm (2.5hz)/160MW, nominal velocity, at a 128hz acquisition frequency. Orbits for X-Y displacements at acquisition points 1,2 and 3 (nodes 6,11 and 16 in the finite element model, respectivelly) are shown in Fig. 9, before and after filtering. The later represents the experimental results caused by rotor unbalancing forces only. In the numerical simulation, time integration was performed with an increment of 5ms. Following CEPEL's information on the system running conditions, a 15 kg.m unbalancing was force at node 5 in the model, - the generator position - which corresponds to the 3700N syncronous force excitation imposed to the model.

In Fig. 10 numerical solutions for the shaft orbits, at the experiment pick up points,

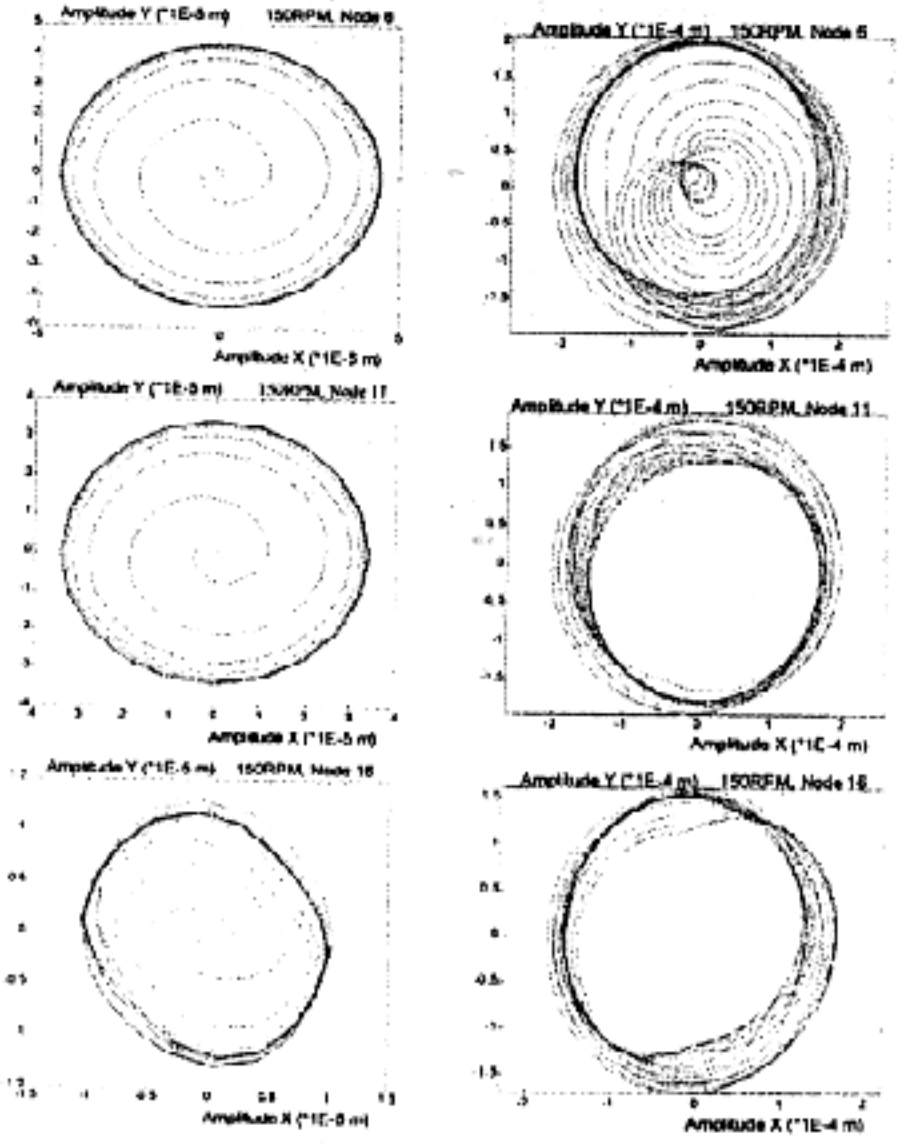

Figure 10 - Numerically Obtained shaft Orbits at the Pick Up Points for Tilting-Pad Journal Assembly (Left) and Plain Journal Assembly (Right)

are compared for two bearing support conditions: the tilting-pad and the plain bearing journals. The finite element representation employed for the shaft, rotor and exciting force is as shown in Fig. 9. It is shown that steady-state running conditions are obtained in both analyses but with differences for the orbit amplitudes: the plain journal bearing model presented orbit amplitudes up to four times the ones obtained from the model with tilting-pad bearing journals. The main reason for such discrepancy is associated to the oil whirl effects presented by the plain bearing model results: spectral displacement values - in both x and y coordinates - at 1.25hz, which is half of the actual rotor rotation frequency (150 rpm).

5. CONCLUSIONS

Numerical procedures to model hydrodynamic bearings, which are compatible to general finite element formulations, for the analysis of rotating systems is presented. Plain hydrodynamic bearings and tilting-pad bearing journals are modeled by closed form obtained stiffness and damping matrices, both reduced to the transverse displacement degrees-of-freedom associated to a single node of the shaft model. Gyroscope effects are also included in the finite element model resulting in a non-symmetric system of equation to be solved for. Althrough the results of some sample solutions indicate the applicability of the proposed procedure for very general situations, further performance studies are still required to identify the limit range of problems for which it can be further employed.

6. REFERENCES

[1] Childs, D., *Turbomachinery Rotordynamics,* Wiley, 1993.

[2] Lalanne, M. and Ferraris, G., Rotordynamics Prediction in Engineering, Wiley, 1998.

[3] Vance, J. M., *Rotordynamics of Turbomachinery*, Wiley, 1988.

[4] Bathe, K. J., *Finite Element Procedures*, Prentice-Hall, 1996.

[5] Nicholas, J. and Barrett, L., The Effect of Bearing Support Flexibility on Critical Speed Prediction. ASLE Transactions, 57(4), 197-207.

[6] Morton, P.G., Influence of Coupled Asymmetric Bearings on The Motion of a Massive Flexible Rotor", Proc. I. Mech Eng., vol. 182, part 1, no. 13, 255-268.

[7] Kirk, R. G. and Gunter, E. S., " The Effect of Flexibility and Damping on the Synchronous Response of a Single Mass Flexible Rotor", ASME Journal of Engineering for Industry, 1972, 221-230.

[8] Rao, J.S., "Sychronous Whirl of a Flexible Rotor in Hydrodynamics Bearings", Mechanism and Machine Theory Journal, vol. 3, no. 12, 1974, 18-28.

[9] Rao, J. S., Bhat, R. B. e Sankar, T. S., "Effect of Damping on the Synchronous Whirl of a Rotor in Hydrodynamic Bearings", Transactions of CSME, vol. 6, no. 3, 1981, 113-121.

[10] Nicholas, J., *A Finite Element Dynamic Analysis of Pressure Dam and Tilting-Pad Bearings,* Ph.D. Thesis, University of Virginia, Charlotteville, VA, 1977.

[11] Hirano, T. and Yamashita, T., "Influence of Bearing Alignment on Vibration of Multi-Span Rotor", DETC'97, ASME Design Engn. Tech. Conf., Sep. 14-17, Sacramento, CA, pp. 1-7, 1997.

[12] Meggiolaro, M. A., Hydrodynamic Bearing Modeling in the Simulation of Rotating Machinery, M.Sc. Thesis, PUC-Rio, August 16th, 1996 (in portuguese).

[13] Cardinali, R., Modeling and Applications in Vertical Rotating Machinery Diagnosis, Ph. Thesis, UNICAMP, 1992.

[14] Capone, G., Descrizione Analítica del Campo di Forze Fluidodinamico Nei Cuscinetti Cilindrici Lubrificati, L'Energia Elétrica, n. 3, pp. 105-110, 1991.

[15] Capone, Cr., "Orbital Motions of Rigid Symmetric Rotor Supported on Journal Bearings", La Meccanica Italiana, v. 199, pp. 37-46, 1986.

[16] Lima, E. N., *"Non-linear model for the Trust Forces in Hydrodynamic Bearings, in Vertical Rotors"*, M.Sc. Thesis, UNICAMP, 1996 (in Portuguese).